Journal of Alloys and Compounds 281 (1998) 202–205

Polytypism in the Nb_3TeI_7 system

Mark D. Smith, Gordon J. Miller*

Department of Chemistry, Iowa State University Ames, Iowa 50011-3111, USA

Received 10 July 1998

Abstract

h-Nb_3TeI_7 represents the first polytype to be observed in a single ternary system of the layered Nb_3QX_7 family (Q=S, Se, Te; X=Cl, Br, I). This compound was synthesized by stoichiometric reaction of the elements at temperatures from 600° to 800°C, and was characterized by single crystal and powder X-ray diffraction. *h*-Nb_3TeI_7 crystallizes in the Nb_3SBr_7 structure type: space group P3m1, a=7.642(1) Å, c=6.897(1) Å and V=348.82(8) $Å^3$. *h*-Nb_3TeI_7 differs from the previously reported polytype, *hc*-Nb_3TeI_7, by having a simpler anion layer stacking sequence involving fewer ${}^2_\infty[Nb_3TeI_7]$ layers per unit cell. Complete structural determinations of the new compound *h*-Nb_3TeI_7 as well as of the previously reported *hc*-Nb_3TeI_7 are included.

Keywords: Niobium chalcogenide halides; Polytypism; Crystal structures

1. Introduction

The layered compound Nb_3TeI_7 was first reported in 1988 by Hönle et al., along with synthetic and crystallographic information for most other members of the family Nb_3QX_7 (Q=S, Se, Te; X=Cl, Br, I) [1]. This family of compounds is closely related to the binary halides Nb_3X_8 [2–4] by simple substitution of a chalcogen atom into the Nb_3X_8 halide matrix, over each Nb_3 cluster. The placement of the chalcogen, and the physical property ramifications of such a substitution have been thoroughly discussed [5]. In turn, both Nb_3X_8 and Nb_3QX_7 are structural derivatives of the CdI_2 type. The CdI_2 type can be considered the parent type of Nb_3X_8 and M_3QX_7, with the latter structures derived from CdI_2 by the introduction of metal-site vacancies, the presence of metal–metal bonding, and the substitution of a chalcogen for a halogen. All three are layered structures, consisting of close-packed anion layers interleaved by planes of metal atoms in every other layer. In the CdI_2 structure, all possible octahedral sites between every other anion layer are occupied, while in Nb_3X_8 and Nb_3QX_7, the Nb atoms order in 3/4 of the octahedral sites between every other layer. The relationship of Nb_3X_8 and Nb_3QX_7 to that of CdI_2 can be illustrated by (conceptually) removing 1/4 of the interstitial metal atoms from the CdI_2 type and drawing the remaining occupied metal sites together into Nb_3 triangular clusters. Nb_3QX_7 can therefore be formulated $Nb_3\square_1QX_7$ (in the case of Nb_3X_8, Q=X). The fundamental metal cluster unit present in Nb_3X_8 and Nb_3QX_7 is the common M_3X_{13} type [6], with the triangular cluster coordinated by one μ_3^i capping atom, three μ_2^i edge-bridging atoms, and nine atoms that provide connections between clusters to create their two-dimensional character.

The reported Nb_3TeI_7 structure is one of five layered structure types known in the Nb_3X_8/Nb_3QX_7 system [5] (a sixth type is formed by Ta_3SBr_7 [7]). These types differ only in the anion layer stacking sequence and relative positions of the metal cluster. Nb_3TeI_7 forms in the Nb_3SeI_7 structure type, space group P6_3mc. This non-centrosymmetric structure consists of an (. . . ABCB . . .) or (. . . *hc* . . .) anion layer stacking sequence, with alternating layers of pure iodide (the 'A' and 'C' layers) and mixed Te/I layers (the 'B' layers). The Nb_3 clusters are inserted between the AB and CB bilayers, such that they are always capped by the tellurium atoms. There are two ${}^2_\infty[Nb_3TeI_7]$ slabs per unit cell, with each successive slab related to the next by a 6_3 screw axis.

Many compounds adopting the CdI_2 structure type are well-known to form polytypes based upon different anion sheet stacking sequences. Therefore, Nb_3QX_7 might also be expected to show polytypism, but up to now this has not been observed. During the course of a study designed to search for such polytypism, we discovered a stacking variant in the Nb_3TeI_7 system. Herein we report the synthesis and structural characterization of this first poly-

---

*Corresponding author.

0925-8388/98/$ – see front matter
PII: S0925-8388(98)00751-8

Table 1
Identification of products from Nb_3TeI_7 reactions at various temperatures

Temp. (°C)	Products	Sample info.
350	*hc*-Nb_3TeI_7 + unreacted intermediates	Powder only
400	*hc*-Nb_3TeI_7	Powder, few crystals
500	*hc*-Nb_3TeI_7	Powder and crystals
600	*h*-Nb_3TeI_7 (minor) + *hc*-Nb_3TeI_7	Several crystals
650	*h*-Nb_3TeI_7 + *hc*-Nb_3TeI_7	Crystalline pieces
700	*h*-Nb_3TeI_7 + *hc*-Nb_3TeI_7 + Nb_3I_8	Crystals
800	*h*-Nb_3TeI_7 + *hc*-Nb_3TeI_7	Crystals
900	No Nb_3TeI_7 phases. Nb_3Te_4 + unknowns	Powder
1025	No Nb_3TeI_7 phases. Nb_3Te_4 + unknowns	Powder

type in the Nb_3QX_7 system. Note: because of the (. . . *hc* . . .) anion layer stacking sequence of the reported Nb_3TeI_7 variant [1], and to distinguish this compound from the new polytype reported here, the Nb_3TeI_7 structure reported earlier (space group $P6_3mc$) will henceforth be referred to as *hc*-Nb_3TeI_7, and the new stacking variant reported below will be labeled *h*-Nb_3TeI_7, in reference to its anion stacking pattern.

2. Experimental

The new polytype *h*-Nb_3TeI_7 was discovered from a study involving a series of reactions of the elements in the ratio 3Nb:Te:7I at nine temperatures ranging from 350°C to 1025°C. Reagents used were: Nb foil (Aesar, 99.995%, washed with a $HF/HNO_3/H_2SO_4$ solution to remove surface impurities, then rinsed with ethanol and dried in vacuo before use); Te (Alfa, 99.99%, thrice-sublimed); I_2 (Alfa, 99.95%, resublimed). All reactions were carried out in evacuated pyrex or fused silica tubes, and the products identified by powder (Guinier camera, Cu Kα) and single-crystal X-ray diffraction. The temperatures used, and the products identified at each temperature are listed in Table 1.

3. Results and discussion

3.1. *hc-Nb_3TeI_7*

A complete structure determination of *hc*-Nb_3TeI_7 has never been reported, only the structure assignment and lattice constants [1]. Crystals of *hc*-Nb_3TeI_7 were proliferate in the various Nb_3TeI_7 reactions carried out as part of this study, therefore a full structure determination is now given. Intensity data from a hexagonal prism selected from a 600°C reaction were collected on a Siemens P4 diffractometer equipped with Mo Kα radiation. After correcting the 1488 collected reflections ($2\theta_{max} = 60°$) for absorption (psi-scans), the structure was easily solved by direct methods [8] using Nb_3SeI_7 as a structural model, and refined with SHELXL-93 [9]. Further crystallographic information is listed in Table 2. Atomic coordinates and isotropic displacement parameters are given in Table 3. Further details of the structure will be discussed in reference to *h*-Nb_3TeI_7.

3.2. *h-Nb_3TeI_7*

The new polytype *h*-Nb_3TeI_7 was first observed from a stoichiometric mixture of the elements heated at 700°C. This tube contained crystals of two visually dissimilar

Table 2
Summary of crystallographic data for *hc*-Nb_3TeI_7

Formula weight	1294.63
Crystal system	Hexagonal
Space group	$P6_3mc$ (No. 186)
Color of crystal	Black
Dimensions of crystal (mm)	0.15×0.15×0.30
Lattice parameters (Å)	
a	7.6300(10)
c	13.800(3)
Vol. ($Å^3$)	695.8(2)
Z	2
d_{calc} ($g\ cm^{-3}$)	6.180
Diffractometer	Siemens P4
Radiation	Mo Kα (λ = 0.71073 Å)
Linear absorption coefficient	19.967 mm^{-1}
Transmission range, max/min.	0.741/0.344
Temperature of data collection	23°C
Scan method	ω scan
Scan speed	Variable: 3 to 60°/min in ω
hkl ranges	$-10 \leq h \leq 1$ $-1 \leq k \leq 10$ $-1 \leq l \leq 12$
$2\theta_{max}$ (deg)	60.00
Number refl. measured	1488
No. unique, observed ($F_o \geq 4\sigma(F_o)$)	283
Weighting scheme	$w^{-1} = \sigma^2(F_o^2) + 0.0399F_c^2$
No. parameters refined	25
Residuals[a]	
$F_o \geq 4\sigma(F_o)$	R1 = 0.0520; wR2 = 0.0959
All data	R1 = 0.0799; wR2 = 0.1065
GoF, all data[b]	1.071
Largest difference peak, $e^-/Å^3$	2.501
Largest difference hole, $e^-/Å^3$	−2.789

[a] $R1 = \Sigma \| F_o| - |F_c \| / \Sigma |F_o|$; $wR2 = [\Sigma[w(F_o^2 - F_c^2)^2] / \Sigma[w(F_o^2)^2]]^{1/2}$.
[b] $GoF = S = [\Sigma[w(F_o^2 - F_c^2)^2]/(n-p)]^{1/2}$, where *n* = no. of reflections, *p* = total no. of parameters refined.

Table 3
Positional parameters and isotropic displacement parameters for *hc*-Nb_3TeI_7

Atom	x	y	z	U_{eq}
Nb	0.8667(2)	$-x$	1/4 (fixed)	0.0112(7)
Te	0	0	0.1022(5)	0.0122(11)
I1	2/3	1/3	0.3563(6)	0.0142(13)
I2	0.1694(2)	$-x$	0.3814(4)	0.0128(6)
I3	0.4979(2)	$-x$	0.1375(5)	0.0147(6)

morphologies. The majority of the crystals were hexagonal prisms. However, many crystals from this tube had a trigonal, or triangular prismatic morphology. The Guinier pattern of samples of these crystals clearly differed from the pattern of the known phase *hc*-Nb_3TeI_7, most diagnostically by the absence of one intense diffraction line. Guinier powder patterns for Cu Kα X-radiation calculated from single-crystal solutions of *hc*-Nb_3TeI_7 and *h*-Nb_3TeI_7 are compared in Fig. 1.

3.3. Structures of h-Nb_3TeI_7 and hc-Nb_3TeI_7

Triangular prismatic shaped crystals of *h*-Nb_3TeI_7 were eventually located from reactions at 600°, 650°, and 700°C. A crystal from the 650°C reaction tube was selected, mounted in a glass capillary under argon, and aligned on a Siemens P4 diffractometer. The initial unit cell was determined on the basis of several reflections located with the aid of a rotation photograph. Axial photographs confirmed the cell edge lengths, and subsequently the unit cell was refined using 40 reflections from $6° \leq 2\theta \leq 25°$. *h*-Nb_3TeI_7 forms in the trigonal system, Laue symmetry 3m1, with $a = 7.642(1)$ Å, $c = 6.897(1)$ Å, and $V = 348.82(8)$ Å^3. A total of 694 reflections were collected to $2\theta_{max} = 50°$, of which 316 were observed. Psi-scans of several reflections for an empirical absorption correction were collected, and later applied to the data. The structure was easily solved by direct methods using SHELXS-86 [8], and refined with SHELXL-93 [9]. Table 4 summarizes other relevant crystallographic data. Atomic coordinates and isotropic displacement parameters are given in Table 5. (A complete listing of all crystallographic data for *hc*-Nb_3TeI_7 and for *h*-Nb_3TeI_7, from both single crystal and powder diffraction data, may be obtained from the authors.)

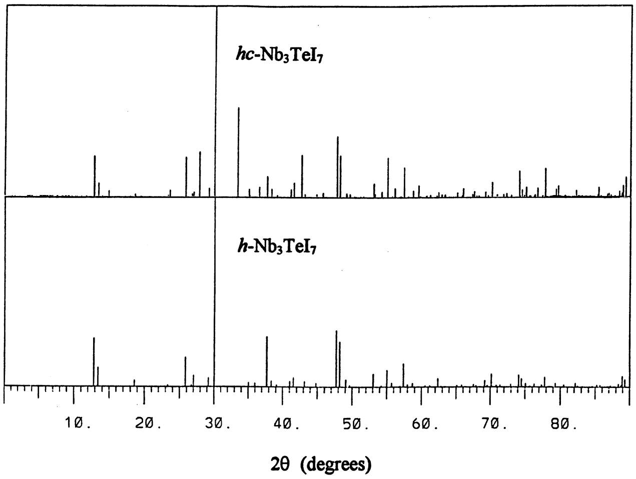

Fig. 1. Comparison of the powder diffraction patterns of *hc*-Nb_3TeI_7 (upper) and *h*-Nb_3TeI_7 (lower). The intense line at $2\theta \approx 33.4°$ in the *hc*-Nb_3TeI_7 pattern is the 203 reflection.

Table 4
Summary of crystallographic data for *h*-Nb_3TeI_7

Formula weight	1294.63
Crystal system	Trigonal
Space group	P3m1 (No. 164)
Color of crystal	Black
Dimensions of crystal (mm)	0.1×0.1×0.2
Lattice parameters (Å)	
a	7.642(1)
c	6.897(1)
Vol. (Å^3)	348.82(8)
Z	1
d_{calc} (g cm^{-3})	6.163
Diffractometer	Siemens P4
Radiation	Mo Kα (λ=0.71073 Å)
Linear absorption coefficient	19.913 mm^{-1}
Transmission range, max/min.	0.922/0.815
Temperature of data collection	23°C
Scan method	ω scan
Scan speed	Variable; 2 to 45°/min in ω
hkl ranges	$-9 \leq h \leq 1$
	$-1 \leq k \leq 9$
	$-1 \leq l \leq 8$
$2\theta_{max}$ (deg)	50.00
Number refl. measured	694
No. unique, observed ($F_o \geq 4\sigma(F_o)$)	316
Weighting scheme	$w^{-1} = \sigma^2(F_o^2) + 0.0317F_c^2$
No. parameters refined	25
Residuals[a]	
$F_o \geq 4\sigma(F_o)$	R1=0.0264; wR2=0.0588
All data	R1=0.0268; wR2=0.0590
GoF, all data[b]	1.211
Largest difference peak, e$^-$/Å^3	1.26
Largest difference hole, e$^-$/Å^3	−3.183

[a] $R1 = \Sigma \| F_o| - |F_c \| / \Sigma |F_o|$; $wR2 = [\Sigma[w(F_o^2 - F_c^2)^2] / \Sigma[w(F_o^2)^2]]^{1/2}$.
[b] $GoF = S = [\Sigma[w(F_o^2 - F_c^2)^2]/(n-p)]^{1/2}$, where n = no. of reflections, p = total no. of parameters refined.

h-Nb_3TeI_7 is the first example of polytypism discovered in the M_3QX_7 system. *h*-Nb_3TeI_7 forms in the Nb_3SBr_7 structure type [1,6], space group P3m1, with one Nb_3TeI_7 slab per unit cell. The anion layer stacking sequence is

Table 5
Atomic coordinates and isotropic displacement parameters for *h*-Nb_3TeI_7

Atom	x	y	z	U_{eq}
Nb	0.86658(9)	$-x$	1/2 (fixed)	0.0095(3)
Te	0	0	0.2015(4)	0.0104(4)
I1	2/3	1/3	0.7129(3)	0.0115(4)
I2	0.16938(8)	$-x$	0.7637(3)	0.0121(3)
I3	0.49855(7)	$-x$	0.2747(3)	0.0135(3)

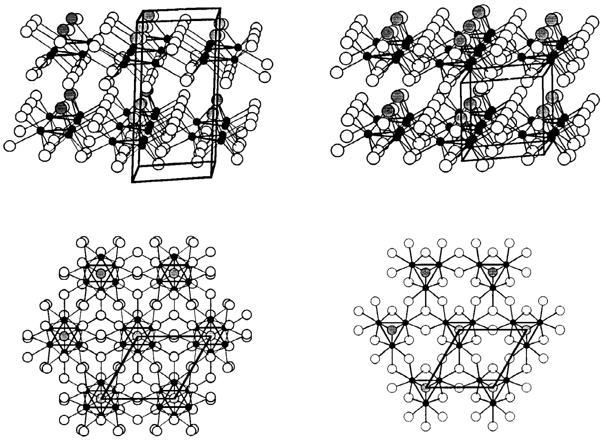

hc-Nb_3TeI_7 *h*-Nb_3TeI_7

Fig. 2. Near-[100] (upper) and [001] (lower) views of the *hc*-Nb_3TeI_7 (left column) and *h*-Nb_3TeI_7 (right column) structures. In all views, two ${}^{2}_{\infty}[Nb_3TeI_7]$ layers and unit cells are shown. Small black circles, Nb; grey circles, Te; open circles, I.

hexagonally close-packed (. . . ABAB . . .), or (. . . *h* . . .), from which derives the nomenclatural choice. The ‘A’ layers are composed of pure I, and the ‘B’ layers of mixed Te/I. Unlike *hc*-Nb_3TeI_7, where each successive ${}^{2}_{\infty}[Nb_3TeI_7]$ layer is related to the next by a 6_3 screw axis, in *h*-Nb_3TeI_7 successive layers are directly ‘superimposed’ on top of one another. Near-[100] and [001] views of these two structure types are shown in Fig. 2. Bond distances and angles for *h*-Nb_3TeI_7 are listed in Table 6, and, as expected, are quite similar to those in *hc*-Nb_3TeI_7, also in Table 6.

It is tempting to speculate on the effect of temperature on the distribution of the two Nb_3TeI_7 polytypes, since a dependence on temperature is observed (Table 1). To wit, *h*-Nb_3TeI_7 seems to be favored at higher temperatures, as it was not observed at temperatures below 600°C. A question of how to assign relative abundances of the two polytypes in these mixtures is apt. Visual estimates are clearly dubious, since the phases often form as large, solid silver plugs whose morphology is not evident, and because taking powder patterns of every bit of material in the tube is impractical. A more sinister complication is how to determine if bulk samples of *hc*-Nb_3TeI_7 contain any *h*-Nb_3TeI_7. Because the simpler *h*-Nb_3TeI_7 pattern is virtually identical to the *hc*-Nb_3TeI_7 pattern except for the absence of a particular line (the 203 reflection in the *hc*-Nb_3TeI_7 pattern, see Fig. 1), *hc*-Nb_3TeI_7 can always be conclusively identified, whereas *h*-Nb_3TeI_7 cannot. If the *h*-Nb_3TeI_7 pattern is superimposed onto the *hc*-Nb_3TeI_7 pattern, it will be undetectable. In order to minimize this problem, small single crystal samples were used whenever possible, but because of their small size, often several crystals or larger samples less likely to be homogeneous were used. Because of this problem, estimates of which phases form at which temperatures are probably skewed in favor of *hc*-Nb_3TeI_7.

Table 6
Selected bond distances (Å) in *h*- and *hc*-Nb_3TeI_7

Bond	*h*-Nb_3TeI_7	*hc*-Nb_3TeI_7
Nb–Nb	3.059(2)	3.052(5)
Nb–Te	2.713(2)	2.695(6)
Nb–I1 (μ_3^a-I)	3.0262(15)	3.023(5)
Nb–I2 (μ_2^i-I)	2.737(2)	2.731(4)
Nb–I3 (μ_2^a-I)	2.9122(12)	2.911(4)

Acknowledgements

This work was supported partially by the Donors to the Petroleum Research Fund, administered by the American Chemical Society, and by the National Science Foundation (DMR-96-27161). We thank Robert Jacobson for use of the diffractometer.

References

[1] W. Hönle, S. Furuseth, G.J. Miller, H.-G. von Schnering, 9th International Conference on Solid Compounds of Transition Elements, Abstracts, Royal Society of Chemistry, London, 1988.

[2] H.-G. von Schnering, H. Wöhrle, H. Schäfer, Naturwissenschaften 48 (1961) 159.

[3] S.S. Berdonosov, A.V. Lapitskii, Russ. J. Inorg. Chem. 10 (1965) 2812.

[4] A. Simon, H.-G. von Schnering, J. Less-Common Metals 11 (1966) 31.

[5] G.J. Miller, J. Alloys Comp. 217 (1995) 5.

[6] G.V. Khvorykh, A.V. Shevelkov, V.A. Dolgikh, B.A. Popovkin, J. Solid State Chem. 120 (1995) 311.

[7] M.D. Smith, G.J. Miller, J. Solid State Chem., in press.

[8] G.M. Sheldrick, ‘SHELXS-86’, Univ. Göttingen, Germany, 1986.

[9] G.M. Sheldrick, ‘SHELXL93 Program for the Refinement of Crystal Structures’, Univ. Göttingen, Germany, 1993.